Self-Assembly of Alkyl-Substituted Polyphenylene Dendrimers on Graphite

Simona Loi,[†] Uwe-Martin Wiesler,[‡] Hans-Jürgen Butt,*[,†] and Klaus Müllen[‡]

Institut für Physikalische Chemie II, Universität Siegen, 57068 Siegen, Germany, and Max-Planck-Institut für Polymerforschung, 55099 Mainz, Germany

Received December 8, 2000

ABSTRACT: The lateral organization of alkyl-substituted polyphenylene dendrimers on the basal plane of graphite has been investigated using atomic force microscopy. The dendrimers consist of a core of twisted, interlocked benzene rings and an external shell of dodecyl chains. Three kinds of dendrimers were used which in solution show a tetrahedral or a disklike shape. On graphite the dendrimers spontaneously form a stable, almost pinhole free monolayer. Complex two-dimensional arrangements and supramolecular ordering were observed in these monolayers prepared by spin-coating. One prominent structure observed with all three dendrimers was regions consisting of parallel rows of 6 nm spacing. In addition, pairs of dendrimers formed two-dimensional crystals on graphite. A simple model to interpret structure formation is discussed. The structure depends sensitively on the structure of the dendrimer, on the solvent, and on the concentration.

Introduction

The adsorption of macromolecules onto solid surfaces is of general interest in order to understand phenomena like ordering, growth, wetting, adhesion, lubrication, and corrosion which are determined by intermolecular, molecule−substrate, and molecule−solvent interactions. Dendrimers are ideal to study this process because they are monodisperse macromolecules with well-defined shape and dimension.[1−4] Another motivation comes from materials science. One challenge in materials science is the creation of supramolecular materials in which the constituent units are highly ordered macromolecules. Small functional units are usually made using macroscopic techniques such as electron beam lithography to form individual microscopic structures (top-down approach). The smaller the structures are, the more complex and expensive the lithographic techniques become. Alternatively, one can form larger units by a spontaneous assembly of molecules (bottom-up approach). Examples are the formation of micelles from surfactants or the formation of biological membranes from lipids. While in the top-down approach individual structures are made sequentially, in the bottom-up approach many similar units are made with little technological effort. Hence, the techniques are complementary, and both will probably be used for the fabrication of functional units with dimensions below 100 nm.

A starting point is the self-assembly of molecules on surfaces. Several molecules are known to self-assemble on solid surfaces as highly ordered, regular structures. Examples are thiols or disulfides on gold[5−7] or several surfactants on silica, graphite, mica, or gold.[8−10] Thin films of several block copolymers form regular structures after annealing or as a melt.[11−14] In contrast, macromolecules usually do not form periodically ordered structures on surfaces. Only a few exceptions are known.[15−18]

In this paper we show that one such exception are polyphenylene dendrimers on graphite. We describe the synthesis of polyphenylene dendrimers and the preparation of self-assembled dendritic monolayers on the basal plane of graphite. With the last generation dodecyl chains were attached to the dendrimer. A formation of dendritic monolayers is possible because the alkyl chains adsorb strongly to graphite; the adsorption energy in gaseous environment is ≈7 kJ/mol per methylene unit.[19] In addition, each phenylene subunit contributes an adsorption energy of ≈15 kJ/mol.[20] The structure of polyphenylene layers on graphite was analyzed with an atomic force microscope (AFM). The purpose of this paper is to describe the different supramolecular structures formed by dendrimers on graphite more than to explain how these structures form. Nevertheless, some conclusions can already be drawn, and a simple model of structure formation is presented.

Experimental Section

Sample Preparation. (a) The Dendrimers. The alkylated polyphenylene dendrimers were synthesized following a general concept described previously.[21−23] A detailed description of the synthesis is described below. First impression about the shape and the size of dendrimers was obtained by molecular mechanic simulations.[21,24] The simulated diameter of the polyphenylene cores of dendrimer **1** and **3**[36] (without alkyl chains) is 3.8 nm. They are shaped like a tetrahedron. The core of dendrimer **2** (without alkyl chains) has a propeller-like shape with a diameter of 3.3 nm. Simulations were confirmed by light scattering[26] and TEM.[27]

(b) Preparation of Dendrimer Layers. The dendrimer layers were prepared with the spin-coating technique. A drop of solution was deposited on a freshly cleaved HOPG (highly oriented pyrolytic graphite) surface, and the sample was immediately rotated at 810 rpm for 10 s. During the rotation time the sample changed its color, indicating the thinning of the film. Dendrimers were dissolved in dichloromethane p.a. at a concentration between 2 μg/mL and 0.2 mg/mL.

(c) Atomic Force Microscopy. Samples were imaged at room temperature with a commercial AFM (Nanoscope III, Digital Instruments, Santa Barbara, CA). For tapping mode we used rectangular silicon cantilevers (Nanosensors, 125 μm long, 30 μm wide, 4 μm thick) with an integrated tip, a nominal

[†] Universität Siegen.
[‡] Max-Planck-Institut für Polymerforschung.
* To whom correspondence should be addressed. Phone +49 271-740 4125; fax +49 271-740 3198; e-mail butt@chemie.uni-siegen.de.

10.1021/ma002090y CCC: $20.00
Published on Web 04/21/2001

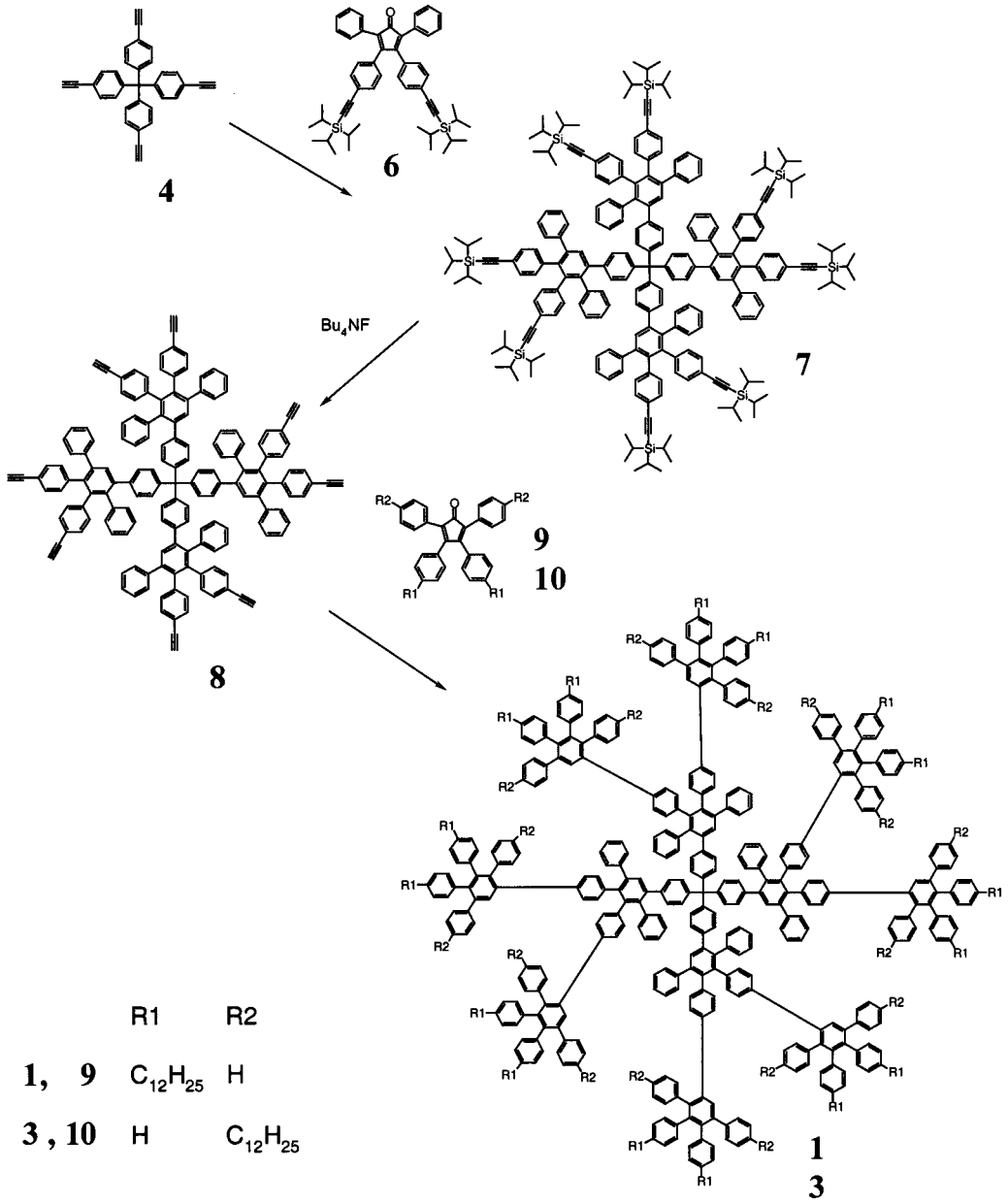

Figure 1. Synthetic pathways for dendrimers **1** and **3**. The attached groups were $R_1 = C_{12}H_{25}$ and $R_2 = H$ for dendrimer **1** and $R_1 = H$ and $R_2 = C_{12}H_{25}$ for dendrimer **3**.

spring constant of 42 N/m, and a resonance frequency of 330 kHz. Contact imaging was done with V-shaped silicon nitride cantilevers (Digital Instruments, 110 μm long, 0.6 μm thick, spring constant roughly 0.11 N/m). The scanner was calibrated laterally by imaging a rectangular grid of 1 μm mesh size and in the *z*-direction as described in ref 28.

(d) Ellipsometry. The thickness of samples was also determined with ellipsometry (ELX-1, DER-Dr. Riss Ellipsometerbau GmbH, operating at $\lambda = 632.8$ nm and at fixed angle of incidence $\varphi = 70°$). Two characteristic angles, Δ and Ψ, were measured. Δ is defined by $\Delta = \delta_1 - \delta_2$, where δ_1 is the phase difference between the parallel component and the perpendicular component for the incoming wave and δ_2 is the same difference for the outgoing wave. Ψ gives the changes for the amplitude and is defined as $tg\Psi = |R^P|/|R^S|$, where R^P and R^S are the total reflection indices for the parallel and the perpendicular component of the polarized light. After a calibration of the ellipsometer through substrate characterization, the polymer film thickness can be calculated from the measured values of Δ and Ψ.

Synthesis of Dendrimers. In the case of dendrimers **1** and **3**, the starting point of the synthesis was the tetrahedric core tetrakis(4-ethynylphenyl)methane (**4**) (Figure 1),[29] whereas in the case of dendrimer **2** 1,3,5-triethynylbenzene (**5**)[30] was used as core (Figure 2). By Diels−Alder cycloaddition of the cores with 3,4-bis(4-triisopropylsilylethynylphenyl)-2,5-diphenylcyclopentadienone (**6**) in refuxing *o*-xylene, the triisopropylsilylethynylated first-generation polyphenylene dendrimers **7** and **11** could be synthesized in quantitative yields. Deprotection of these dendrimers with tetrabutylammonium fluoride in THF gave the ethynyl-substituted dendrimers **8** and **12** also in quantitative yields. The alkylated dendrimers **1** and **3** were synthesized by Diels−Alder cycloaddition of **8** with the dodecyl alkylated tetraphenylcyclopentadienones **9** and **10**. Dendrimer **2** was obtained by the cycloaddition of **12**. After isolation by column chromatography dendrimers **1**, **2**, and **3** were obtained as white powders, with good solubility in solvents like THF, chloroform, toluene, or hexane and thermal stability to temperatures higher than 300 °C. Characterization, done by NMR and MALDI-TOF mass spectrometry, allowed to check the purity and monodispersity of each step of the synthesis. Dendrimers **1**, **2**, and **3** were therefore obtained as monodisperse macromolecules with molecular masses of 7579 and 5522 g/mol, respectively.

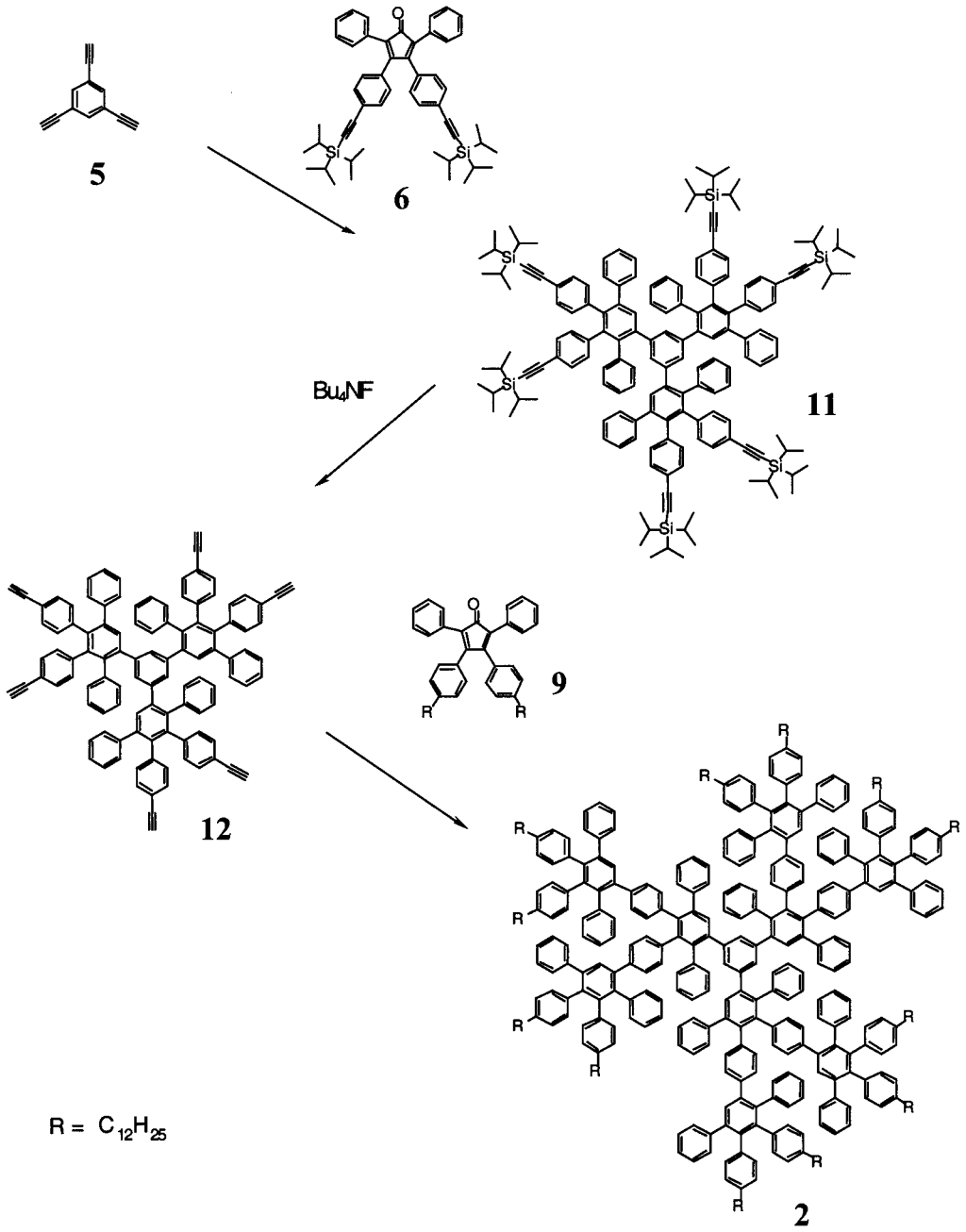

Figure 2. Synthetic pathway for dendrimer **2**. The rest groups R were dodecyl chains ($C_{12}H_{25}$).

(a) Materials. All starting materials were obtained from commercial suppliers (Aldrich, Fluka, Fischer, Strem, Acros, Riedel de Haen) and were used without purification. Solvents were used in HPLC grade purity as purchased. Flash chromatography was carried out with silica gel 60 (230−400 mesh) from E. Merck. ^{1}H and ^{13}C NMR spectra were recorded on a Bruker DRX 500 and a Bruker AMX 300 spectrometer. Mass spectral analyses were carried out on ZAB2-SE-FPD (VG Analytical) and Bruker Reflex-TOF spectrometers. MALDI-TOF mass spectra were measured using a 337 nm nitrogen laser and 1,8,9-trihydroxyanthracene as matrix. Elemental analyses were obtained on a Foss Heraeus vario EL.

(b) Diels−Alder Cycloaddition of Ethynyl- and Tetraphenylcyclopentadienone Derivatives. A mixture of ethynyl derivative and 1.5 molar equiv of tetraphenylcyclopentadienone derivative per ethynyl bond was refluxed for 10 h in 10 mL of *o*-xylene per gram of the starting materials under an argon atmosphere. After reaction the solvent was removed in vacuo, and the crude product was purified by reprecipitation or column chromatography.

(c) Desilylation of Triisopropylsilylethynyl Derivatives. A solution of 2 molar equiv of ammonium fluoride per TiPS group to be removed and 40 mmol of the trialkylsilyl derivative were dissolved under argon in 100 mL of tetrahydrofuran. To the solution was added 4 mmol of *n*-tetrabutylammonium fluoride dissolved in 10 mL of tetrahydrofuran. The end of the reaction was determined by TLC (silica gel). This was usually the case after 2 h. The solution was then diluted with 500 mL of dichloromethane and extracted with distilled water. The organic phase was removed, washed with 400 mL of 6 M hydrochloric acid followed by 400 mL of distilled water, and dried over magnesium sulfate. The solvents were removed in vacuo, and the crude product was purified by reprecipitation or column chromatography.

^{1}H NMR (300 MHz, TDF, 303 K): δ_H (ppm) = 7.50 (s, 4H); 7.44, 7.38 (s, 8H); 7.22−7.00 (m, 60H); 6.98−6.42 (m, 172H); 2.35 (t, 32H; $H_{CH2-\alpha}$); 1.58−1.04 (m, 320H; H_{CH2}); 0.89 (t, 48H; $H_{CH2-\omega}$). ^{13}C NMR (75 MHz, TDF, 303 K): δ_C (ppm) = 145.5, 143.1, 142.9, 141.9, 141.7, 141.3, 141.2, 140.6, 140.5, 140.4, 140.3, 140.3, 140.1, 140.0, 139.9, 139.6, 139.1, 138.9, 138.8,

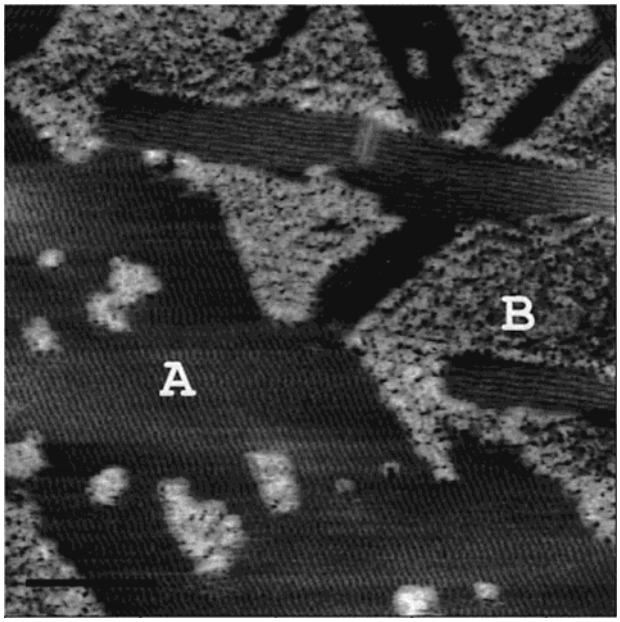

Figure 3. Image (450 × 450 nm; scale bar 100 nm) of dendrimer **1** layers on HOPG imaged in tapping mode prepared from a solution of 2 μg/mL dendrimer in dichloromethan. The letters "A" and "B" indicate the nanorod and the diffuse structure, respectively.

138.6 (C_{quat}); 132.6, 132.3, 132.0, 131.8, 131.2, 130.7, 129.5, 129.3, 128.2, 127.6, 127.3, 126.8, 126.2 (C_{tert}); 36.2 ($C_{aliph\alpha}$); 32.8, 32.1, 30.6, 30.6, 30.4, 30.3, 29.8, 29.7, 23.5 (C_{aliph}); 14.4 ($C_{aliph\omega}$). MALDI-TOF mass spectrum: *m/e*: 7618.5 (100%, $[M, K]^+$, calcd 7618.67). Elemental Anal. Calcd for $C_{577}H_{644}$: C, 91.44; H, 8.56. Found: C, 94.16; H, 5.41.

^{1}H NMR (300 MHz, TDF, 303 K): δ_H (ppm) = 7.52 (s, 4H); 7.47, 7.42 (s, 8H); 7.36−6.42 (m, 232H); 2.58−2.32 (m, 32H; $H_{CH2-\alpha}$); 1.64−1.04 (m, 320H; H_{CH2}); 0.98−0.78 (m, 48H; $H_{CH2-\omega}$). ^{13}C NMR (75 MHz, TDF, 303 K): δ_C (ppm) = 145.5, 142.9, 142.8, 142.7, 142.0, 141.8, 141.7, 141.6, 141.4, 141.2, 140.6, 140.5, 140.4, 140.2, 140.1, 140.1, 139.9, 139.9, 139.7, 139.1, 138.8, 138.5 (C_{quat}); 132.5, 132.0, 131.8, 131.2, 130.9, 130.6, 129.6, 129.3, 128.3, 127.8, 127.5, 127.2, 126.1, 125.8 (C_{tert}); 36.3, 36.2 ($C_{aliph\alpha}$); 32.8, 32.3, 30.6, 30.4, 30.3, 30.2, 29.8, 23.5 (C_{aliph}); 14.5, 14.4 ($C_{aliph\omega}$). MALDI-TOF mass spectrum: *m/e*: 7618.0 (100%, $[M, K]^+$, calcd 7618.67). Elemental Anal. Calcd for $C_{577}H_{644}$: C, 91.44; H, 8.56. Found: C, 94.16; H, 5.41.

^{1}H NMR (300 MHz, TDF, 303 K): δ_H (ppm) = 7.42, 7.38 (s, 8H); 7.24−6.30 (m, 174H); 2.44−2.28 (m, 24H; $H_{CH2-\alpha}$); 1.54−1.04 (m, 240H; H_{CH2}); 0.89 (t, 36H; $H_{CH2-\omega}$). ^{13}C NMR (75 MHz, TDF, 303 K): δ_C (ppm) = 143.0, 142.8, 141.9, 141.7, 141.5, 141.3, 141.2, 141.1, 140.4, 140.3, 140.1, 139.9, 139.3, 138.9, 138.7, 138.6 (C_{quat}); 132.6, 132.3, 132.0, 131.7, 131.0, 130.7, 130.4, 129.5, 129.2, 128.2, 127.6, 127.3, 126.7, 126.2 (C_{tert}); 36.1 ($C_{aliph\alpha}$); 32.8, 32.1, 30.6, 30.6, 30.4, 30.3, 29.8, 29.7, 23.5 (C_{aliph}); 14.4 ($C_{aliph\omega}$). MALDI-TOF mass spectrum: *m/e*: 5524.8 (100%, $[M]^+$, calcd 5522.46). Elemental Anal. Calcd for $C_{420}H_{474}$: C, 91.44; H, 8.56. Found: C, 94.16; H, 5.41.

Results

Layers Prepared from Low Concentrated Dendrimer 1. When preparing dendrimer **1** layers from a low concentrated solution (2 μg/mL), the whole surface was covered with a continuous layer. Different types of packing structures were observed (Figure 3). One of the most remarkable structures were regions covered by parallel rows of 6 ± 1 nm spacing ("nanorods" or type A structure). Usually type A regions were elongated along the rows. They tended to align parallel or at angles of 60° or 120° with respect to each other. This indicates that they are oriented by the underlying graphite lattice.

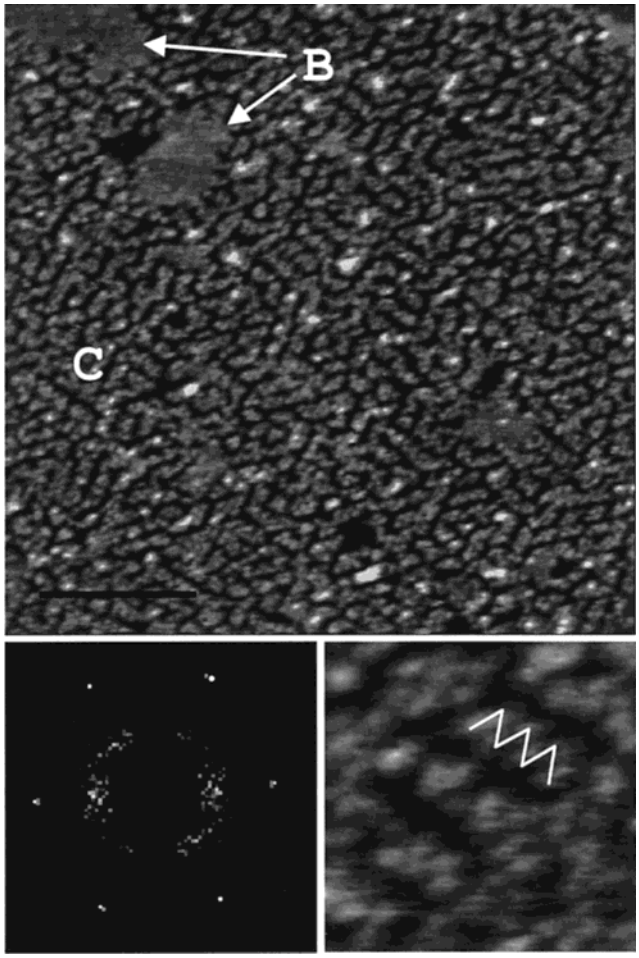

Figure 4. (top) Dendrimer **1** monolayer on HOPG imaged in tapping mode prepared from a 20 μg/mL dichloromethane solution. Image size: 410 × 410 nm; scale bar 100 nm. Light areas are high and dark regions are low. The letters "B" and "C" indicate type B (homogeneous) packing structure and type C (stripped) structure. (bottom) A detail of 51 × 51 nm (right) and a two-dimensional Fourier transform (left).

In addition, we observed extended diffuse regions (type B). These diffuse regions were not bare graphite but were covered with a relatively homogeneous layer of dendrimers. Other parts of the surface were covered with a wormlike structure (type C, not shown). The distance between neighboring "worms" was roughly 11 nm. The areas covered by type A, B, and C structures varied from sample to sample. Nanorods (type A) were observed in 11 out of 17 experiments. Considering all experiments, roughly 15% of the surface was covered by structure A, 82% by type B, and 3% by type C structure.

Dendrimer 1 Layers Prepared from Higher Concentrated Solutions. Two different kinds of packing structures were observed when preparing layers from 20 μg/mL solutions (Figure 4). Roughly 90% of the surface was covered by stripes or wormlike structures of 11 nm spacing. (We call it type C, like for layers prepared from low concentrated solutions.) The spacing was deduced from the distance between neighboring stripes. Hence, a broadening of the lateral dimension due to the tip shape convolution with that of the dendrimer is negligible. The stripes showed a tendency to oriented parallel (0°), 60°, or 120° with respect to each other. They seem to consist of rows of dendrimers arranged in a zigzag (Figure 4, right, bottom). A two-

dimensional Fourier transform shows six reflexes at angles of 60 ± 4° corresponding to a distance of 6.0 ± 0.2 nm. This indicates that on average the dendrimers are located at the sites of an hexagonal lattice with a lattice constant of 6.9 ± 0.3 nm = 6.0 nm/sin 60°. The area per unit cell of the hexagonal lattice is 41 nm^2. Hence, each unit cell probably contains one molecule. The maximal area occupied by one dendrimer can be estimated from the length of an extended polyphenylene chain with 10 subunits plus two dodecyl chains that is roughly 7 nm. At hexagonal close packing circles of 7 nm diameter would occupy an area of 42 nm^2. This value agrees with the area of the unit cell.

The remaining 10% of the surface was covered with a completely homogeneous layer (type B) of constant height. Only few holes were observed, and little area was not covered at all. Hence, the dendrimers form an almost pinhole free layer.

In monolayers changes in the structure were observed (Figure 5). At the time scale required to take an image (typically 10−20 min) stripes disintegrate into more circular blobs, and the individual blobs realign into new stripes. This change in structure is not necessarily accompanied by a long-range lateral diffusion of the individual dendrimers. It merely reflects that a dendrimer which is positioned between two neighbors shifts from one neighbor to the other one (see also Figure 15).

Thickness of Layers. We measured a thickness from 0.7 to 1.5 nm for dendrimer layers formed from 20 μg/mL solution while the diameter of the molecules, as obtained from computer simulations, is 5.5 nm. The thickness was determined in three ways (results are listed in Table 1). First, from cross sections of images that include a hole in the layer (Figure 6a). Second, from cross sections of areas that include a region that has been scraped free before (Figure 6b). To scrape the graphite free, an area was scanned roughly 5 times in contact mode at a force of 100−200 nN. (Scanning with forces significantly higher than 200 nN destroyed the HOPG structure, and much deeper holes were formed.) Hence, the results indicate that the dendrimers change their shape when adsorbing to graphite and probably are "flattened" on the surface.

To verify this with an independent method as a third technique ellipsometry was used, although the accuracy is lower than with the AFM. Knowing the refractive index and the absorption index for HOPG (n_g = 2.55 and k_g = 1.42) and assuming a refractive index of n = 1.6 for the dendrimer layer, a difference of Δ between the HOPG and the sample of 2° corresponds to a thickness of 1.5 ± 0.7 nm. The refractive index for polystyrene is n = 1.59. We assume that this value is similar to the refractive index for the dendrimers. If we change n by 0.1, the derived thickness should have an error of ≈14%. We could not use the Ψ value because it varied too weakly as a function of the thickness for our system.

The observed self-assembled structure of polyphenyl dendrimers is specific in the sense that it was only observed in air (which we think is representative for gaseous environment), on HOPG, and when formed from a solution of dichloromethane. When immersing samples in ethanol, images show that the molecules are able to regain the three-dimensional shape that they have in solution and to assume an average height of roughly 7 nm (Figure 7). Ethanol competes for binding sites to the graphite, and it is a solvent for the dendrimers. Both effects weaken the adsorption of dendrimers to graphite. Being only weakly adsorbed, dendrimer **1** regained is original tetrahedral shape that leads to aggregates of 7 nm height.

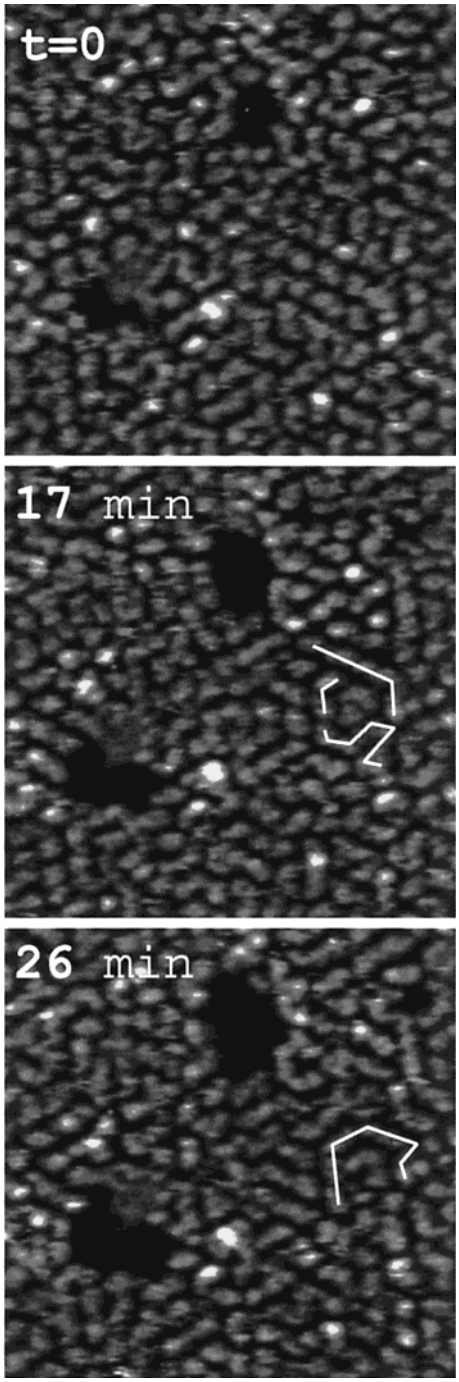

Figure 5. Sequence of images (200 × 200 nm, scale bar 50 nm) of dendrimer **1** layer on graphite prepared from a 20 μg/mL dichloromethane solution. Some changes between the last two images are indicated by lines.

Table 1. Thickness Values Determined from Cross Sections of Images That Contained a Hole, from Scraping a Hole in the Layer, and with an Ellipsometer[a]

	dendrimer **1**	dendrimer **2**	dendrimer **3**
cross section [nm]	0.8 ± 0.2	0.8 ± 0.2	0.9 ± 0.2
scratch [nm]	0.7 ± 0.3	1.0 ± 0.2	1.1 ± 0.3
ellipsometry [nm]	1.5 ± 0.7	1.6 ± 1.3	1.7 ± 1.1

[a] The samples were prepared from 20 μg/mL concentrated solutions. The errors are the random errors of the mean.

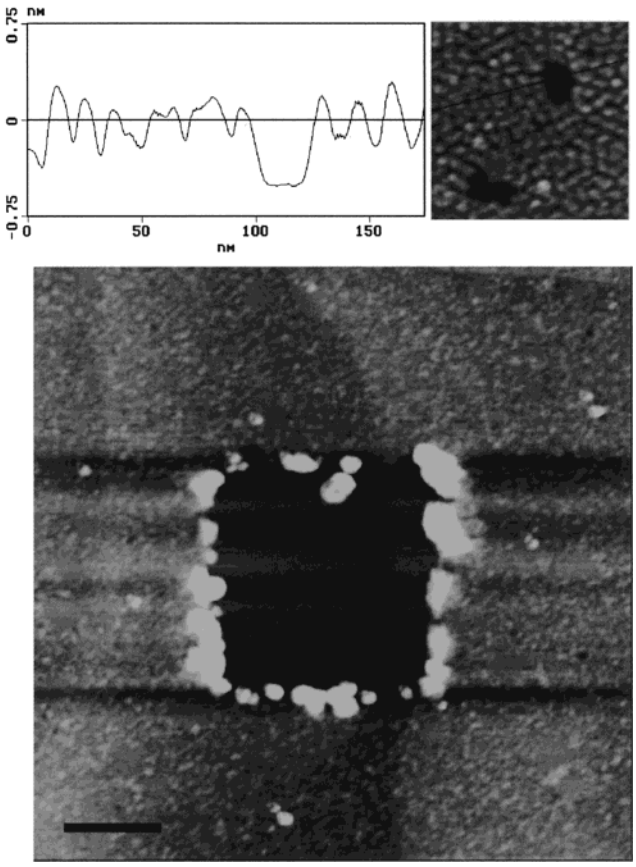

Figure 6. (a, top) Typical cross section through a layer of dendrimer **1** at 20 μg/mL concentration on HOPG. (b, bottom) Tapping mode image (1.5 × 1.5 μm; scale bar 250 nm) of a layer of dendrimer **1** on HOPG. The square in the middle was scraped free by imaging that area five times in contact mode with a force of ≈200 nN.

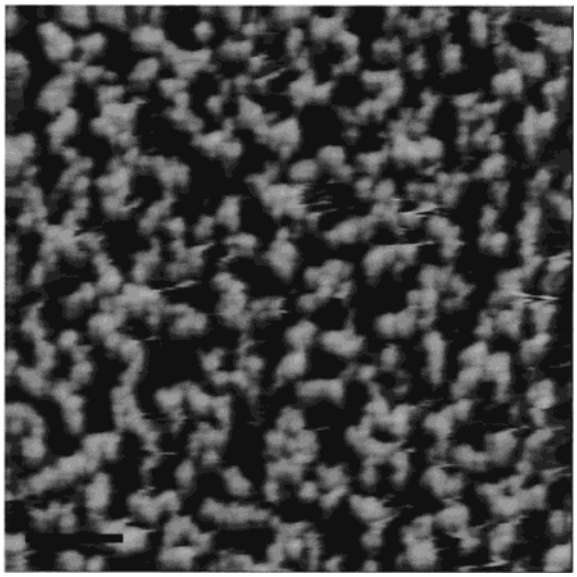

Figure 7. Contact mode image (1.4 × 1.4 μm; scale bar 250 nm) taken in ethanol of a dendrimer **1** layer on HOPG at 20 μg/mL. The sample was prepared as usual and then immersed in ethanol.

The structures type A, B, and C are thermodynamically stable. Annealing at 96 °C for 30 min in a oven did not change them. One difference was, however, the occurrence of 0.1−2 μm long needlelike objects on top of the monolayer (Figure 8). Their height and width were typically 1.5−2.0 and 10 nm, respectively. On many samples such needles formed from dendrimers were observed even without annealing. After annealing, however, their number increased drastically.

Figure 8. Large-scale tapping mode image (2 × 2 μm; scale bar 500 nm) of a layer of dendrimer **1** prepared from a dichloromethane solution (20 μg/mL) after annealing the sample at 96 °C for 30 min.

Figure 9. AFM tapping-mode image of a sample prepared from a 20 μg/mL solution of dendrimer **1** dissolved in dichlorobenzene on graphite (5 × 5 μm; scale bar 1 μm).

To check the effect of the solvent, we prepared layers with dendrimers dissolved in dichlorobenzene instead of dichloromethane. We observed clusters of a defined height (≈5 nm) while the rest of the graphite surface was covered with a homogeneous diffuse layer (Figure 9). On the top of the cluster we could observe a granular structure, but the molecules did not arrange in any ordered structure. A possible interpretation of the images is that the solvent could adsorb stronger than the dendrimers to the graphite and hinder the formation of an ordered dendrimer layer. The structure and the height of the clusters did not change even after annealing the sample at 150 °C for 30 min.

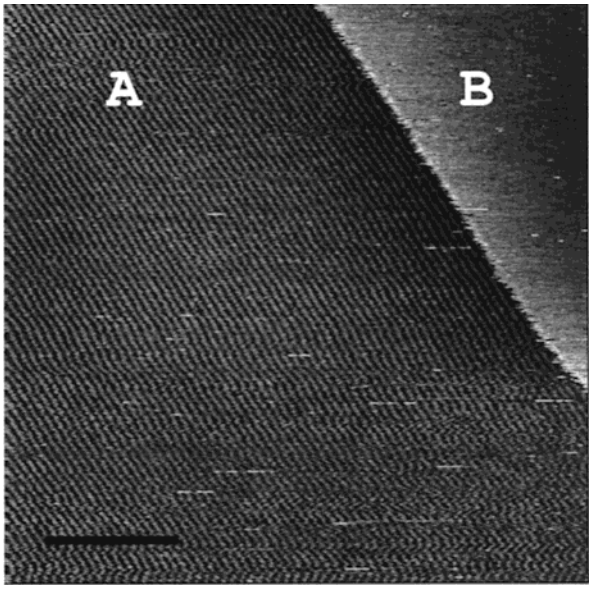

Figure 10. Tapping mode image of a monolayer of dendrimer **3** on graphite prepared from low-concentration solution (2 μg/mL dichloromethane). Image size 438 × 438 nm, scale bar 100 nm. The rows are 6 nm apart.

Preparing samples from high concentrated solutions (0.2 mg/mL), we obtained layers of 3−5 nm thickness as determined from scratching experiments (image not shown here). No individual dendrimers could be identified anymore, and no regular structures were observed.

Structure of Monolayers Prepared from Dendrimer 3. Dendrimers **1** and **3** are different only for the position of the alkyl chains that in dendrimer **3** are substituted more inside while in dendrimer **1** they are all at the surface of the polyphenylene moiety. Samples prepared from a low-concentration solution (2 μg/mL) of dendrimer **3** show two different structures (Figure 10): regions covered with parallel rows of 6 nm spacing (type A) and regions covered with a homogeneous layer of defined height (type B). The rows were not stable and often disappeared after scanning them several times.

When preparing dendrimer **3** layers from a higher concentrated solution (20 μg/mL), we observed a uniform layer with only few holes. It was possible to distinguish single molecules. The molecules were, however, not as clear as in layers of dendrimer **1**, and they did not form ordered structures. Hence, the clear distinction between an inner phenylene core and an outer alkyl shell which characterized dendrimer **1** is probably important for the formation of lateral structures.

The thickness of the layers was 0.8−1.6 nm (Table 1). Comparing this value with the diameter in solution of 5.5 nm, we conclude that dendrimers **3** also flatten on the graphite surface. The positions of the alkyl chains do not change the flattening of the molecules on the surface.

Structure of Layers Prepared from Dendrimer 2. Dendrimer **2**, with its central benzene group, has a more planar, propeller-like shape with an height of roughly 2 nm as deduced from computer simulations. When preparing samples of dendrimer **2** from a 2 μg/mL concentrated dichloromethane solution, in four of six experiments two-dimensional crystals were formed (Figure 11). We determined the lattice constants as described before.[31] The primitive unit cell could be described by the lattice constants $a = 7.4 \pm 0.4$ nm, $b = 10.1 \pm 0.3$ nm, and an angle of $121 \pm 2°$. Crystals

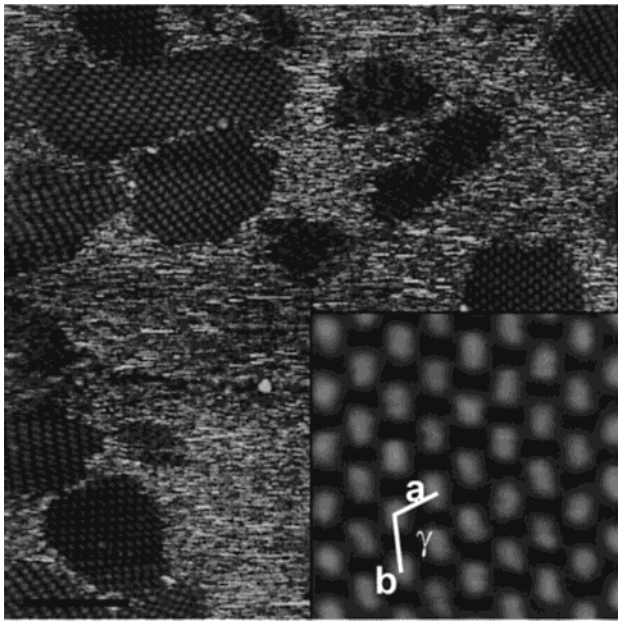

Figure 11. Dendrimer **2** layer formed from 2 μg/mL concentrated dichloromethane solution (580 × 580 nm, scale bar 100 nm). (top) The molecules form two-dimensional crystals. (bottom right) A detail of a crystal lattice. The lattice vectors are indicated.

were oriented parallel (0°) or 60° or 120° with respect to each other, indicating that the underlying graphite determines their orientation. Each unit cell probably contained at least two molecules. This is indicated by the area of a unit cell of 63 nm^2. The calculated diameter of a molecule is roughly 6.5 nm, which leads to a value for the area per molecule of 35.5 nm^2. Considering that this is an upper limit, this value agrees with the experimental one. In addition, each protrusion in a unit cell had an elongated, oval, and not spherical shape. This shows that supramolecular structures are formed at different levels: first, two dendrimers form pairs, and then these pairs form a two-dimensional crystal.

The two-dimensional crystals were stable and could be scanned many times. We observed, however, changes in the period of time required to take an image (Figure 12): crystalline regions changed their shape and size. Some even disappeared or changed their alignment.

In one experiment we observed rod formation as with dendrimer **1**. The spacing between the rods was again 6 nm. The rods were not stable and disappeared after scanning them few times (Figure 13). Afterward, the area was covered by a diffuse structure.

Discussion

Self-Assembled, Supramolecular Structures. The results show that alkyl-substituted polyphenylene dendrimers form self-assembled and supramolecular structures on graphite: "self-assembled" in the sense that they form patterns fast (within 1−5 s) and spontaneously even from low concentrated solutions and they are stable; "supramolecular" in the sense that the structure is complex and not easily predictable like a hexagonal close packing. Formation of rods on surfaces has been observed from dendritic nanorods.[32] However, to our knowledge this is the first observation of rod formation from the self-assembly of approximately spherical or circular nanometer-sized macromolecules. The fact that strongly adsorbed macromolecules form complex two-

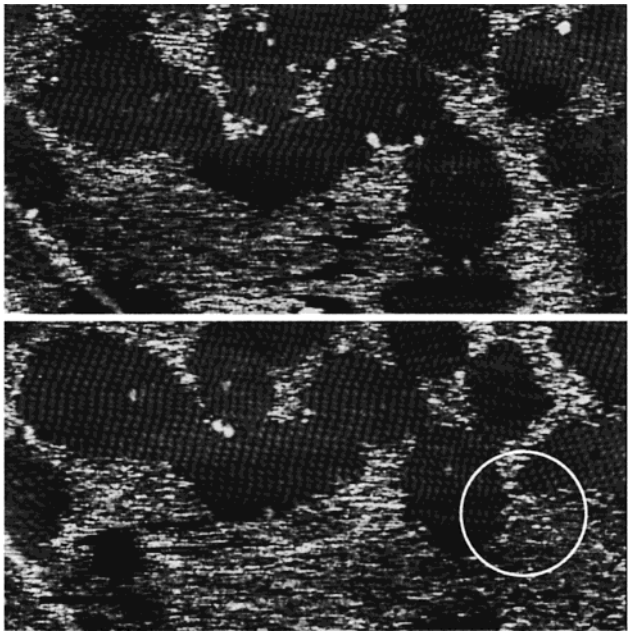

Figure 12. Two subsequent images (573 × 573 nm, scale bar 100 nm) of dendrimer **2** layer prepared from 2 μg/mL solution. After 10 min it is possible to notice changes in the shape and extension of the two-dimensional crystals. The circle for instance shows the same area on the sample. The position, shape, and size of crystalline areas have changed.

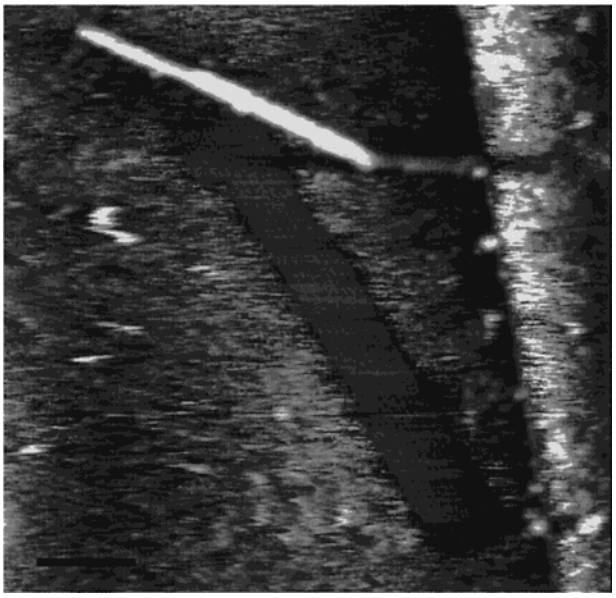

Figure 13. Dendrimer **2** layer prepared from 2 μg/mL dichloromethane solution (615 × 615 nm, scale bar 100 nm). A region consisting of parallel rows with a spacing of 6 nm can be seen.

dimensional patterns on a surface is a surprising observation. A prerequisite for the formation of pattern or two-dimensional crystals is probably that the dendrimers are able to diffuse laterally.

Thickness of the Layers. The measured thickness values show that the dendrimers change their shape when adsorbing to graphite. The tetrahedral shape of dendrimers **1** and **3** is lost, and the dendrimers lay flat on the surface. A reduced thickness of dendrimer layers on solid surfaces was observed before.[33,34] For the dendrimers to lay flat on the surface the oligophenol chains have to bend. This requires energy because oligophenylene chains are relatively stiff. This energy is available since the adsorption energy of the alkyl chains is high. A single dodecyl chain has an adsorption energy of ≈80 kJ/mol.[19] Even considering that the first few methylenes next to the phenylene moiety are sterically hindered to bind directly to the graphite, the adsorption energy of the alkyl chains of one of the four arms of a dendrimer is roughly 200 kJ/mol. In addition, each phenylene ring contributes an adsorption energy of about 15 kJ/mol,[35] irrespective of whether it is oriented parallel or perpendicular to the graphite surface. This leads to an adsorption energy of 225 kJ/mol per arm, if it lays flat on the graphite. Such a high available energy could be enough to bend the oligophenylene chains.

Mobility of Dendrimers. Before considering the conformation of the dendrimers on the graphite surface, we would like to stress that single dendrimers on bare graphite are probably to a certain degree mobile. Hydrocarbon chains are strongly adsorbed to graphite, and once they are adsorbed it is unlikely that they leave the surface spontaneously. They can, however, diffuse laterally. Computer simulations of individual alkyl chains on graphite revealed negligible activation energy for the translation along the chain.[19] Hence, probably the dendrimers can diffuse on bare graphite. This mobility explains that we were never able to get images of half-covered graphite. We observed either a totally bare graphite surface or an almost pinhole free dendrimer monolayer. On the partially covered surface the AFM tip pushes the dendrimer to the side so that they are not detectable. They have to be stabilized in a monolayer in order to become visible for the AFM.

Circular-Disk Model. To interpret the images as a zero-order approximation, we consider the dendrimers **1** on graphite as circular disks with a core of roughly 4 nm diameter consisting of the phenylene moiety and an outer region formed by the alkyl chains. Two neighboring dendrimers repel each other as soon as the outer regions start to overlap. The reason is that the number of possible conformations an alkyl chain can assume on the graphite is restricted because of the presence of a neighboring dendrimer. This causes an entropically driven repulsion. To estimate the possible entropy loss an alkyl chain undergoes when being confined, we first calculate the entropy of an alkyl chain of n monomers. We assume that the positions of the first two monomers are fixed and determined by the position of the polyphenylene core. In bulk there are three possible positions for the third methylene unit, corresponding to the trans and two gauche configurations. On a surface only two positions are possible, assuming that the methylene units are in contact with the surface. The fourth methylene unit can assume two positions (for each of the two conformations of the third subunit). Then n subunits can assume 2^{n-2} conformations. The entropy is $S = k_B \ln 2^{n-2} = (n - 2)k_B \ln 2$. For the difference in free enthalpy between a totally confined and a free alkyl chain on graphite, we obtain

$$\Delta G = T\Delta S = (n - 2)k_B \ln 2$$

assuming that there are no energy differences between the configurations. For $n = 12$ this exceeds the thermal energy $k_B T$ significantly. Hence, the entropic repulsion can influence the structure of dendrimers on graphite. Considering that the high adsorption energy leads to a relatively high density of dendrimers and taking the entropic repulsion into account, one expects a hexagonal

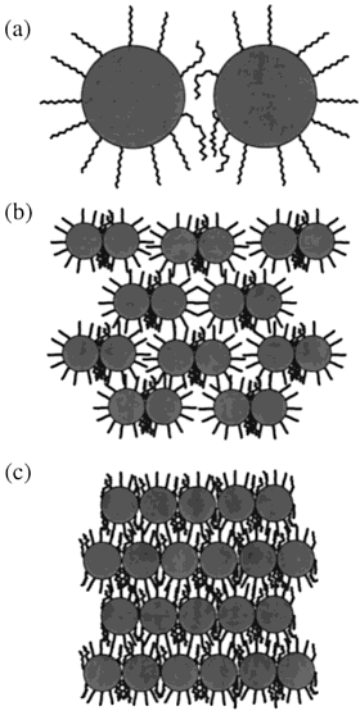

Figure 14. (a) Schematic drawing of two dendrimers approaching each other on a graphite surface. The gray circles represent the polyphenylene core. The alkyl chains are drawn as zigzag lines extending from the core. (b) The close-packed structure of pairs which is similar to the two-dimensional crystalline region observed. (c) Row formation of dendrimers.

packing. The hexagonal structure is the densest way to arrange circular disks which cannot overlap or which repel each other on a surface.

On the basis of the circular disk model, the average hexagonal packing of type C structure can be understood. Still, two obvious questions arise:

(1) Why do the dendrimers also form others structures such as rows (type A) or two-dimensional crystals (dendrimer **2**)? The reason is probably that more dendrimers fit onto the surface when they assume these particular structures. If for instance some alkyl chains interdigitate, the area per molecules is reduced. A loss entropy is overcompensated by the energy gain due to the adsorption energy. One could only speculate about the precise structure because atomic resolution information is missing. Experiments with the scanning tunneling microscope were not successful.

(2) Why do we never observe larger, regular aggregates with coordination numbers higher than 2? The coordination number is the number of nearest neighbors that are in direct contact. Since the two-dimensional crystalline regions are formed by a close packing of pairs of dendrimers **2**, the coordination number is 1. In regions with parallel rows (type A) the coordination number is 2. Even in the zigzag structure (type C) the coordination number is probably 2.

We think that due to the entropic repulsion of the peripheral alkyl chains, an anticooperative binding between dendrimers on a surface is observed. When two dendrimers approach each other on the graphite surface, the alkyl chains between the two dendrimers are squeezed out of the gap between them (Figure 14a). They will, however, remain on the surface because the adhesion energy is so high. This increases the number of alkyl chains at both sides of the pair, and the entropic repulsion toward a third dendrimer increases. Such an effect could stabilize pairs of molecules and explain the two-dimensional crystalline structure (Figure 14b). If a third dendrimer is force into contact with a pair, it is most likely to approach from the end of a pair because there the number of alkyl chains is still relatively low. This effect favors the formation of rows (Figure 14c). Then, however, the number of alkyl chains on both sides of the row is so high that no other dendrimer can get into contact with the row. In this way type A structures can be rationalized.

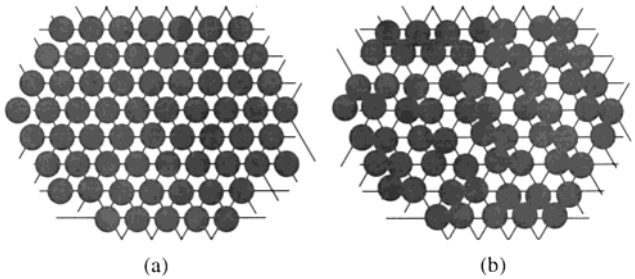

Figure 15. Sketch of the two-dimensional structure expected for dendrimer **1** at 0.02 mg/mL concentration (a). At average each dendrimer occupies one site of a hexagonal lattice. Because of the short-range attraction, it is shifted toward one or at most two neighbors (b).

The same argument is probably important to understand the zigzag structure (type C). A sketch of the two-dimensional structure expected from the circular-disk model is depicted in Figure 15a. Each dendrimer occupies one site of a hexagonal lattice. Because of the high adsorption energy, some dendrimers are force together to form pairs (Figure 15b). Stripes consisting of dendrimers arranged in a zigzag, and pairs of dendrimers appear. This model is also consistent with the observed changes in the structure of type A (Figure 4).

At this point it is necessary to address one question concerning the two-dimensional fast Fourier transform (2DFFT) of images of dendrimer **1** films. How can stripes with a zigzag arrangement of molecules, which at first sight do not show a periodic ordering and which might be formed as depicted in Figure 15b, lead to distinct spots in the 2DFFT? An argument similar to the reasoning in X-ray crystallography is used. Sharp reflexes are obtained in X-ray diffraction patterns of crystals although the individual molecules thermally fluctuated. Quantitatively this is included in the Debye−Waller factor (Kittel, Festkörperphysik, S. 665). In our case the dendrimers also "fluctuate" around their lattice sites, not in time but in space. Each dendrimer might be displaced from his lattice site, but on average they form a hexagonal lattice. A simple mathematical treatment is described in the Appendix.

An open question is the influence of the underlying graphite lattice. Type A and C structures are probably aligned by the graphite lattice. Otherwise, it is difficult to understand why the stripes or rows tend to form angles of 0°, 60°, or 120° with respect to each other. We cannot deduce from our model whether the orientation is caused by the alkyl−graphite interaction or by the interaction of the phenol moiety with the graphite.

Acknowledgment. We thank D. Johannsmann for helping us to with the ellipsometer measurements. We are also grateful to Jürgen Rabe and Paolo Samori, Berlin, who did the STM measurements with us. The

project was supported by the Deutsche Forschungsgemeinschaft Graduiertenkolleg "Physik und Chemie supramolekularer Systeme" (S.L.) and the Fonds der Chemischen Industrie (U.-M.W.). We also acknowledge the financial support of the Bundesministerium für Bildung und Forschung (03C0299 7).

Appendix. Two-Dimensional Fourier Transform Expected from a Hexagonal Lattice with Randomly Displaced Molecules

We first assume that each dendrimer has the same height and size in an AFM image. Hence, all dendrimers contribute equally to the two-dimensional Fourier transform (2DFFT), and the "scattering factor" f is the same for each dendrimer. This is not totally true. Even if all dendrimers have identical shapes in an AFM image, they might appear differently. This difference is due to the tip influence. If a single molecule is imaged by an AFM tip, its volume appears enlarged since the image is something like a convolution between tip and sample. If two dendrimers that are in contact are imaged, the volume in the image is less than twice the volume of a single dendrimer because the enlargement is effective only on one side. This effect, that due to the tip shape neighboring dendrimers appear with a reduced volume, is neglected.

We consider the structure of dendrimers as described in Figure 15b. On average, the dendrimers are positioned at a certain place in the hexagonal unit cell. This position is given by the two-dimensional vector $\vec{r}_0$. This vector goes from the origin of the unit cell to the mean position of the dendrimer. Each dendrimer is shifted a discrete distance Δ toward one of its neighbors. The shift is directed along one of the six lattice axes. Though only a certain discrete shift distance is allowed, the direction of the shift is supposed to be random; i.e., a shift along each of the six axis has the same probability.

The intensity of a reflex in the 2DFFT (corresponding to the scattering amplitude) is proportional to the square of the structure factor, F_{hk}, which is given by

$$F_{hk} = \frac{f}{A} \exp(-i\vec{G}_{hk}\vec{r})$$

A is the area of a unit cell. $\vec{G}_{hk}$ is the reciprocal lattice vector for the reflexes with Miller indexes h and k. With the unit vectors in real space $\vec{a}$ and $\vec{b}$ the unit vectors in reciprocal space, $\vec{A}$ and $\vec{B}$, are defined by

$$\vec{A}\cdot\vec{a} = 2\pi, \quad \vec{A}\cdot\vec{b} = 0, \quad \vec{B}\cdot\vec{a} = 0, \quad \vec{B}\cdot\vec{b} = 2\pi$$

An AFM image contains typically 1000−10 000 dendrimers. Hence, the 2DFFT averages over a large number of molecules. The average structure factor is

$$F_{hk} = \frac{f}{A} \langle \exp(-i\vec{G}_{hk}\vec{r}) \rangle$$

We assume that $\vec{r} = \vec{r}_0 + \vec{u}$, with $|\vec{u}| = \Delta$. The direction of $\vec{u}$ is along one of the six lattice axes. Inserting leads to

$$F_{hk} = \frac{f}{A} \exp(-i\vec{G}_{hk}\vec{r}_0) \langle \exp(-i\vec{G}_{hk}\vec{r}) \rangle$$

We write the last factor in a series:

$$\langle \exp(-i\vec{G}_{hk}\vec{r}) \rangle = 1 - i\langle \vec{G}_{hk}\vec{u} \rangle - \frac{1}{2}\langle (\vec{G}_{hk}\vec{u})^2 \rangle \pm \ldots$$

The displacement in each of the six directions is random and not correlated with the reciprocal lattice vector. Hence, the second term is zero. For the last term we can write

$$\langle (\vec{G}_{hk}\vec{u})^2 \rangle = {G_{hk}}^2 \langle u^2 \rangle \langle \cos^2 \varphi \rangle$$

Since the displacement is supposed to be discrete, the second term is $\langle u^2 \rangle = \Delta^2$. φ is the angle included by the reciprocal lattice vector and $\vec{u}$. If the angle between say $\vec{a}$ and $\vec{G}_{hk}$ is denoted by φ_0, the angles with the other five axes are $\varphi_0 + \pi/3$, $\varphi_0 + 2\pi/3$, $\varphi_0 + \pi$, $\varphi_0 + 4\pi/3$, and $\varphi_0 + 5\pi/3$. Since a displacement in all six directions has the same probability, we get

$$\langle \cos^2 \varphi \rangle = \frac{1}{6}\left[\cos^2 \varphi_0 + \cos^2\left(\varphi_0 + \frac{\pi}{3}\right) + \ldots + \cos^2\left(\varphi_0 + \frac{\pi}{3}\right)\right] = \frac{1}{2}$$

Hence, we obtain

$$\langle \exp(-i\vec{G}_{hk}\vec{u}) \rangle = 1 - \frac{1}{4}{G_{hk}}^2\Delta^2 \pm \ldots$$

Using this expression, the intensity of the inner six reflexes (characterized by h and k = 1, 0 or 0, 1 or 1, 1) is

$$I = I_0 \exp\left(-2\pi^2\frac{\Delta^2}{a^2}\right)$$

The exponential factor corresponds to the Debye−Waller factor. Here, a is the lattice constant of the hexagonal lattice. In summary, the intensity of the inner spots decreases exponentially with the relative displacement Δ/a squared.

References and Notes

(1) Orr, G. W.; Barbour, L. J.; Atwood, J. L. *Science* **1999**, *285*, 1049−1052.
(2) Schenning, A. P. H. J.; Elissen-Roman, C.; Weener, J. W.; Baars, M. W. P. L.; van der Gaast, S. J.; Meijer, E. W. *J. Am. Chem. Soc.* **1998**, *120*, 8199−8208.
(3) Berresheim, A. J.; Müller, M.; Müllen, K. *Chem. Rev.* **1999**, *99*, 1747−1785.
(4) Percec, V.; Ahn, C. H.; Ungar, G.; Yeardley, D. J. P.; Möller, M.; Sheiko, S. S. *Nature* **1998**, *391*, 161−164.
(5) Strong, L.; Whitesides, G. M. *Langmuir* **1988**, *4*, 546−558.
(6) Poirier, C. *Chem. Rev.* **1997**, *97*, 1117−1127.
(7) Nelles, G.; Schoenherr, H.; Jaschke, M.; Wolf, H.; Schaub, M.; Küther, J.; Tremel, W.; Bamberg, E.; Ringsdorf, H.; Butt, H.-J. *Langmuir* **1998**, *14*, 808−815.
(8) Manne, S.; Gaub, H. E. *Science* **1995**, *270*, 1480−1482.
(9) Jaschke, M.; Butt, H.-J.; Gaub, H. E.; Manne, S. *Langmuir* **1997**, *13*, 1381−1384.
(10) Ducker, W. A.; Wanless, E. J. *Langmuir* **1999**, *15*, 160−168.
(11) Stocker, W.; Beckmann, J.; Stadler, R.; Rabe, J. P. *Macromolecules* **1996**, *29*, 7502−7507.
(12) Meiners, J. C.; Elbs, H.; Ritzi, A.; Mlynek, J.; Krausch, G. *J. Appl. Phys.* **1996**, *80*, 2224−2227.
(13) Binder, K. *Adv. Polym. Sci.* **1999**, *138*, 1−89.
(14) Liu, Y.; Zhao, W.; Zheng, X.; King, A.; Singh, A.; Rafailovich, M. H.; Sokolov, J.; Dai, K. H.; Kramer, E. J.; Schwarz, S. A.; Gebizlioglu, O.; Sinha, S. K. *Macromolecules* **1994**, *27*, 4000−4010.
(15) Rinia, H. A.; Kik, R. A.; Demel, R. A.; Snel, M. M. E.; Killian, J. A.; van der Eerden, J. P. J. M.; de Kruijff, B. *Biochemistry*, in press.
(16) Stawasz, M. E.; Sampson, D. L.; Parkinson, B. A. *Langmuir* **2000**, *16*, 2326−2342.
(17) Hellmann, J.; Hamano, M.; Karthaus, O.; Ijoro, K.; Shimomura, M.; Irie, M. *Jpn. J. Appl. Phys.* **1998**, *37*, L816−L819.

(18) Cui, G.; Xu, Y.; Liu, M.; Fang, F.; Ji., T.; Chen, Y.; Li., Y. *Macromol. Rapid Commun.* **1999**, *20*, 71−76.
(19) Hentschke, R.; Schürmann, B. L.; Rabe, J. P. *J. Chem. Phys.* **1992**, *96*, 6213−6221.
(20) Vernov, A.; Steele, W. A. *Langmuir* **1991**, *7*, 3110−3117.
(21) Morgenroth, F.; Kubel, C.; Mullen, K. *J. Mater. Chem.* **1997**, *7*, 1207−1211.
(22) Morgenroth, F.; Reuther, E.; Mullen, K. *Angew. Chem., Int. Ed. Engl.* **1997**, *36*, 631−634.
(23) Morgenroth, F.; Berresheim, A. J.; Wagner, M.; Mullen, K. *Chem. Commun.* **1998**.
(24) Brocorens, P.; Zojer, E.; Cornil, J.; Shuai, Z.; Leising, G.; Mullen, K.; Bredas, J. L. *Synth. Met.* **1999**, *100*, 141−162.
(25) Loi, S.; Wiesler, U. W.; Butt, H. J.; Müllen, K. *Chem. Commun.* **2000**, 1169−1170.
(26) Fytas, G., personal communication.
(27) Wiesler, U.-M.; Berresheim, A. J.; Morgenroth, F.; Lieser, D.; Müllen, K. *Macromolecules*, submitted.
(28) Jaschke, M.; Butt, H.-J. *Rev. Sci. Instrum.* **1995**, *66*, 1258−1259.
(29) Mongin, O.; Gossauer, A. *Tetrahedron Lett.* **1996**, *37*, 3825−3828.
(30) Weber, E.; Hecker, M.; Koepp, E.; Orlia, W.; Czugler, M.; Csoregh, I. *J. Chem. Soc., Perkin Trans. 2* **1988**, 1251−1257.
(31) Jaschke, M.; Schönherr, H.; Wolf, H.; Butt, H.-J.; Bamberg, E.; Besocke, M. K.; Ringsdorf, H. *J. Phys. Chem.* **1996**, *100*, 2290−2301.
(32) Stocker, W.; Karakaya, B.; Schürmann, B. L.; Rabe, J. P.; Schlüter, A. D. *J. Am. Chem. Soc.* **1998**, *120*, 7691−7695.
(33) Tsukruk, V. V.; Rinderspacher, F.; Bliznyuk, V. N. *Langmuir* **1997**, *13*, 2171−2176.
(34) Takada, K.; Diaz, D. J.; Abruna, H. D.; Cuadrado, I.; Casado, C.; Alonso, B.; Moran, M.; Losada, J. *J. Am. Chem. Soc.* **1997**, *119*, 10763−10773.
(35) Vernov, A.; Steele, W. A. *Langmuir* **1991**, *7*, 2817−2820.
(36) The numbering for the different dendrimers refers to our brief communication (ref 25).

MA002090Y